ADVANCED THEORY AND SIMULATIONS
www.advtheorysimul.com

General Model for Charge Carriers Transport in Electrolyte-Gated Transistors

*Marcos Luginieski, Marlus Koehler, José P. M. Serbena, and Keli F. Seidel**

A charge carrier transport model able to describe the typical modes of operation and some non-ideal ones from electrolyte-gated field effect transistors and organic electrochemical transistors (OECTs) is proposed. The analysis include the effect of 2D or 3D percolation transport (PT) and the influence of a shallow exponential trap distribution on the transport. Under these considerations, a non-constant accumulation layer thickness along the channel can be formed, resulting in a non-constant effective mobility. The accumulation thickness can depict 2D or 3D PT or even a transition between them. This transition can produce a non-ideal profile between the linear and saturation regimes in the output curve, region in which a lump appears. Other analyzed phenomenon is the non-linear behavior for low drain voltage in the output curve, even considering an ohmic contact. This phenomenon is attributed to the traps distribution profile into the semiconductor and the thin accumulation layer thickness close to the injection contact. The conditions when the linear field effect mobility is higher or lower than the saturation one is also analyzed. Finally, electrolyte-gated organic field effect transistors and OECT experimental data are successfully fitted with this model showing its versatility.

1. Introduction

There are many well established phenomenological models to describe the charge carrier transport in field effect transistors (FETs).[1] When such models are extended to organic field effect transistors (OFETs) or even to electrolyte-gated transistors (EGTs), new kinds of theoretical schemes were proposed by adapting models originally developed for silicon-based FETs.[2–5] General phenomenological models that encompass the peculiarities of OFETs or EGTs are more uncommon in the literature. Specifically about EGTs, their theoretical description is more complex since those devices have two distinguished typical modes of operation: i) transconductance due to field effect only, being named as electrolyte-gated organic field effect transistors (EGOFETs) or due to ii) ionic current being named as organic electrochemical transistors (OECTs). In spite of that, it is a common practice in the literature to extract the EGOFET parameters by using approaches based on OFET models.[2]

Furthermore, there are theoretical approaches specifically created for EGOFETs, for example, a model based on the Nernst–Plank–Poisson equation.[3] This model spatially maps the concentration of electrons and ions, together with the distribution of electric potential and field along the transistor channel. The drain current is obtained from the integration of the electrical current density over the length of the channel. In addition, the model brings a quite interesting analysis of the charge densities over the entire device, as well as geometric effects of gate electrode size. Unfortunately, it does not provide an analytical equation for the drain current that can be straightforwardly compared to experiments, and does not allow transient analysis of the output current. It also has the additional disadvantage to be based on non-free software. For OECTs, one of the main used descriptions was proposed in 2007 by Bernards and Malliaras,[4] where the doping or de-doping level is expressed through a volumetric analysis of the organic semiconductor modeled by a gate capacitance (C_G). Their model is based on two simple circuits: an electronic and an ionic. The electronic reflects basically the simple ohmic equations that are the base of OFET models. The ionic part is based on an equivalent circuit, where a resistor in series with a capacitor describes the whole ionic behavior. An extension from the literature[6] was proposed by Paudel et al.,[6] in 2022, based on a 2D drift-diffusion model and showing the importance of considering two distinct time constants transient response to describe the ions movement perpendicular and along the transistor channel on the output current in OECTs.[6] Faria et al.[7] also proposed

M. Luginieski, K. F. Seidel
Universidade Tecnológica Federal do Paraná - UTFPR
Departamento Acadêmico de Física
Av. Sete de Setembro, 3165, Curitiba CEP 80230-901, Brazil
E-mail: keliseidel@utfpr.edu.br
M. Luginieski
Instituto de Física de São Carlos
Universidade de São Paulo
Departamento de Física e Ciências dos Materiais
CP 369, São Carlos, SP CEP 13660-970, Brazil
M. Koehler, J. P. M. Serbena
Universidade Federal do Paraná - UFPR
Centro Politécnico, Departamento de Física
Jardim das Américas CP 19044, Curitiba CEP 81531-990, Brazil
The ORCID identification number(s) for the author(s) of this article can be found under https://doi.org/10.1002/adts.202200852

DOI: 10.1002/adts.202200852

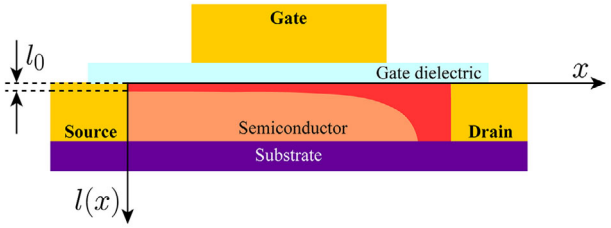

Figure 1. Field effect transistor architecture with bottom contact and top gate and its accumulation thickness variation along the semiconductor channel length (dark red highlights) into the channel. l_0 is the minimum effective thickness.

an analytical model based on an equivalent circuit[7] with the advantage of allowing the extraction of macroscopic parameters such as the capacitance, by simple fits of experimental transient current curves.

All these proposed theories are specifically applied (or adapted) to OECTs or EGOFETs, but they do not have a common general approach since the extraction of characteristic parameters from electrolyte-gated transistors still depends on a priori assumption of the operation mode. It happens since the cited literature as refs. [2–7] take into account some peculiarities in their mathematical description of phenomena. As already mentioned, EGOFETs are described based on models developed for transistors modulated by field effect only, assuming that the effects are similar even with an electrolyte layer into the device. These models are developed based on the premise that the current does not have a time dependence with the movement of ions during the sweeping voltage and that the accumulation layer extends along all the semiconductor thickness. From this approach, it is possible to extract typical macroscopic parameters (as mobility, threshold voltage, transconductance, etc.), in order to quantify the transistor efficiency as well as giving rise to a quantitative interpretation of the phenomena. In OECTs, most of the models seek to understand the transient current during the diffusion of ions into the channel. It means, they are looking for a deterministic function to describe the channel's ionic doping and de-doping dynamics. In most of these models, the temporal analysis does not allow the extraction of the typical macroscopic parameters, despite having successful cases that manage to extract some parameters.[7] Still, some of the models propose the existence of a volumetric capacitance due to the diffused ions into the semiconductor film, not being the same assumption used in EGOFETs. Clearly, the premises of each model are distinctive.

Here we propose that some of those gaps can be filled by considering a model for an injection-based surface field effect transistors (IFETs).[8] The architecture of the IFET is comparable to thin film transistors (TFTs) or OFETs as shown in **Figure 1**. The model analyzes the charge transport by considering the competition between charge carrier trapping at an exponential distribution of traps and the transport improvement produced by the formation of 2D or 3D percolation pathways along the channel. The exponential distribution of traps is related to an energy scale. It comes from an approximation profile of the tail of a Gaussian distribution where there is a low density of localized states, causing these levels to behave like shallow traps. The influence of these two effects was introduced on the effective mobility that is equivalent to the field effect mobility, given by[8]

$$\mu_{\text{eff}} \propto \left(D - D_c\right)^{\alpha} D^{-(\gamma-1)}, \quad D \geq D_c \tag{1}$$

where α is a parameter correlated to the dimension of the percolation pathways, D_c a minimum thickness of the accumulation layer necessary to establish a percolation pathway between source and drain, and D the thickness of the semiconductor film. Necessarily, Equation (1) is valid only when $D > D_c$. α can assume values between 1–1.4 for 2D percolation transport (PT) and 1.5–2 for 3D PT.[8,9] The parameter γ in Equation (1) represents the energetic depth of the exponential distribution of traps. Traps have homogeneous spatial distribution into the channel (interface and bulk in x and y directions). It is usually written as $\gamma = T_c/T$, where T_c is the characteristic temperature of the trap distribution, and T is the temperature. Equation (1) was written by assuming the mobility in a percolative problem with D following then a power law of the kind $\mu_{\text{eff}} \propto (D - D_c)^{\alpha}$.[8] On the other hand, the mobility in the conducting islands decreases with increasing film thickness following also a power law of the kind $\mu_{\text{eff}} \propto D^{-(\gamma-1)}$. This dependence is due to the trap-limited transport within the island, so that the mobility decreases with the increasing number of traps in thicker layers. Hence, the mobility rise due to improved island contacts with increasing D can be partially compensated by the poor transport in those islands.

Another phenomenon known in FETs and EGTs literature is that the accumulation layer does not necessarily occupies the entire thickness of the semiconductor film,[8,10] which can be particularly important in EGTs because these devices have a high capacitance per unit area produced by the electrolyte dielectric film. The density of induced charges at the semiconductor/dielectric surface is then high even at low applied voltages. Due to this key feature, a proper modeling of the charge transport in EGT must take into account the effects produced by variations in the thickness of the accumulation layer (l) with the gate voltage. Since l might abruptly change from just a few nanometers up to the entire thickness of the semiconductor film with voltage variation, it is expected that the gate voltage can induce transitions on the regime of transport. The percolation pathways between source and drain can then present a transition from 2D to 3D transport for a determined voltage, for instance. Such transition might also have a complex behavior produced by the competition between this effect (gauged by the parameter α in Equation (1)) and the trap filling process that depends on γ.

In this way, the present work expands and extends the analysis initially developed in ref. [8] to derive a single model for EGTs. From that model, it is possible to obtain valuable information on typical parameters that controls the behavior of those transistors, using a unique theoretical framework to study the EGOFETs and OECTs modes of operation. In addition to the typical macroscopic parameters analyzed, from the present model it is also possible to infer: i) the profile of the accumulation layer thickness that does not necessarily extend along all the semiconductor film; ii) when the linear mobility is higher or lower than the saturation one (or vice-versa); iii) the non-constant field effect mobility dependent on accumulation layer thickness ($\mu_{\text{eff}}(l)$); iv) the non-linear regime in the output curve even when there is an ohmic-contact;

v) peculiar profiles in the output curve attributed to the transition from 2D to 3D percolation transport.

2. Theoretical Model

The model is reasoned for a transistor architecture as depicted in Figure 1 with bottom contacts and top gate. We are mainly interested in properly describe the charge transport effects associated with the variations on the thickness of the accumulation layer (l) along the channel. Ref. [8] initially addressed the problem to calculate l by solving the drift–diffusion and 1D Poisson equations along the y-direction (the direction is perpendicular to the semiconductor/dielectric interface, see Figure 1). They assumed equilibrium condition under the gradual channel and trap-free approximations. Since the component of the electric-field in the y-direction is much more intense than the component in x-direction, the electric potential (V) is then a function of the direction parallel to semiconductor/dielectric interface (x-direction).[8,11] Those assumptions implies that the current flow occurs only along the plane parallel to the electrolyte/semiconductor interface. As a result, the effective thickness of the accumulation layer ($l(x)$) is a function of $V(x)$ at a coordinate x in the channel

$$l(x) = \begin{cases} \left(\dfrac{V_{tr}}{V_G - V_T - V(x)} \right) D, & V(x) < V_{sat} - V_{tr} \\ D, & V(x) \geq V_{sat} - V_{tr} \end{cases} \quad (2)$$

where $V_{sat} \equiv V_G - V_T$, V_T is the threshold voltage, V_G the gate voltage, $V_{tr} \equiv 4\epsilon kT_c/eC_iD$, ϵ is the electrical permittivity of the semiconductor and C_i is the capacitance per unit area of the gate dielectric. The variation of $l(x)$ as a function of $V(x)$ is schematically illustrated in Figure 1 where the dark red profile filling the channel represents the accumulation layer. At the source region, $V(0) = 0$ V, the thickness of the accumulation layer has its minimum value (called minimum effective thickness), given by $l_0 = D\{V_{tr}/V_{sat}\}$.

In ref. [8] the interplay between the percolation and the trap-filling process to determine the effective mobility (μ_{eff}) of an IFET was written as a function of the entire semiconductor thickness (D). In an EGTs, however, it is expected that the accumulation layer does not necessarily extend along the entire D, but remains concentrated near the semiconductor/dielectric interface for a wide range of voltage operation. It is then reasonable to introduce an effective mobility that depends on the thickness of the accumulation layer by writing μ_{eff} as a function of l instead of D in Equation (1), where l is given by Equation (2)

$$\mu_{eff}(l_x) = \mu_{sat}\left[\frac{(l - D_c)}{D}\right]^{\alpha}\left(\frac{l}{D}\right)^{-(\gamma-1)}, \; D_c < l \leq D \quad (3)$$

where μ_{sat} is the field effect mobility in the saturation regime given by a constant so that $\mu_{eff} = \mu_{sat}$ when $l = D \gg D_c$. The above equation is defined for $l > D_c$ since the charge transport between source and drain is only possible if there is at least one percolation path linking both electrodes.

The first power-law on the right hand side of Equation (3) models the fact that the number of percolation paths connecting the source and drain electrodes tends to increase with l. As the accumulation layers get thicker, the charge carriers populate a greater volume of the organic semiconductor's film. As a consequence, the probability that the carrier will reach a low resistance pathway (able to circumvent the resistive domains produced by the film's imperfections) increases.

On the other hand, the second power-law on the right hand side of Equation (3) models the charge transport in regions free of morphological imperfections but with traps exponentially distributed in energy. Again, as the volume of the accumulation layer grows, the number of traps that can limit the transport (at a specific energy) also increases. This effect tends to reduce μ_{eff} with l (see Equation (19) of ref. [8]).

From the conditions in Equation (2), the μ_{eff} determined by Equation (3) is valid when $V(x) < V_{sat} - V_{tr}$. On the other hand, when $V(x) > V_{sat} - V_{tr}$, the effective mobility has a constant value

$$\mu_{eff}(l = D) = \mu_{sat}\left(\frac{D - D_c}{D}\right)^{\alpha} \quad (4)$$

The drain current for a device illustrated in Figure 1 is calculated from the density of free charge carriers induced in the channel by V_G, or $|dq| = |C_i\, W(V_{sat} - V(x))dx|$,[2] where W is the channel width. One can also write $I_D = dq/dt = (dx/dt) \times (dq/dx) = \mu_{eff}(dV/dx)(dq/dx)$, where μ_{eff} is the ratio between the charge carriers' velocity and the component of the electric field along the x-direction. The expression of the drain current is then[2,8]

$$I_D = \frac{WC_i}{L}\int_0^{V_D} \mu_{eff}(l)[V_G - V_T - V(x)]dV \quad (5)$$

Equation (5) can be calculated as a function of V_D or V_G to give the device's output or transfer typical curves, respectively. Since the field effect mobility is not constant in this model, the integration of Equation (5) must be performed taking into account the two limits settled by Equation (2).

For simplicity (without loss of generality), we are going to assume that the device in Figure 1 works only when positive bias is applied to the source/gate electrodes (it means, an n-type EGT). The **linear regime** of operation is established when $V_D < V_{sat}$. The integration of Equation (5) for this regime gives

$$I_D = \frac{\mu_{sat}C_iW}{LD^{\alpha}}\left[V_{tr}^{-(\gamma-1)}\| + \left(D - D_c\right)^{\alpha}\mathrm{ff}\right] \quad (6)$$

where the $\|$ in Equation (6) is defined as

$$\|(V^*) = D^{\alpha}\int_0^{V^*}\left[\frac{V_{tr}}{V_{sat} - V(x)} - \frac{D_c}{D}\right]^{\alpha}[V_{sat} - V(x)]^{\gamma}dV \quad (7)$$

The integral in Equation (7) cannot be solved analytically, so it needs to be solved numerically. The limit of integration (V^*) in this equation depends on the voltage $V'' = V_{sat} - V_{tr}$: if $V_D < V''$, $V^* = V_D$ otherwise $V^* = V''$. Finally, the ff in Equation (6) is a function of V_D and V'', that is

$$\mathrm{ff}(V'', V_D) = \theta(V_D - V'')\left[V_{sat}(V_D - V'') - \frac{V_D^2 - V''^2}{2}\right] \quad (8)$$

where $\theta(V_D - V'')$ is the Heaviside's step function.

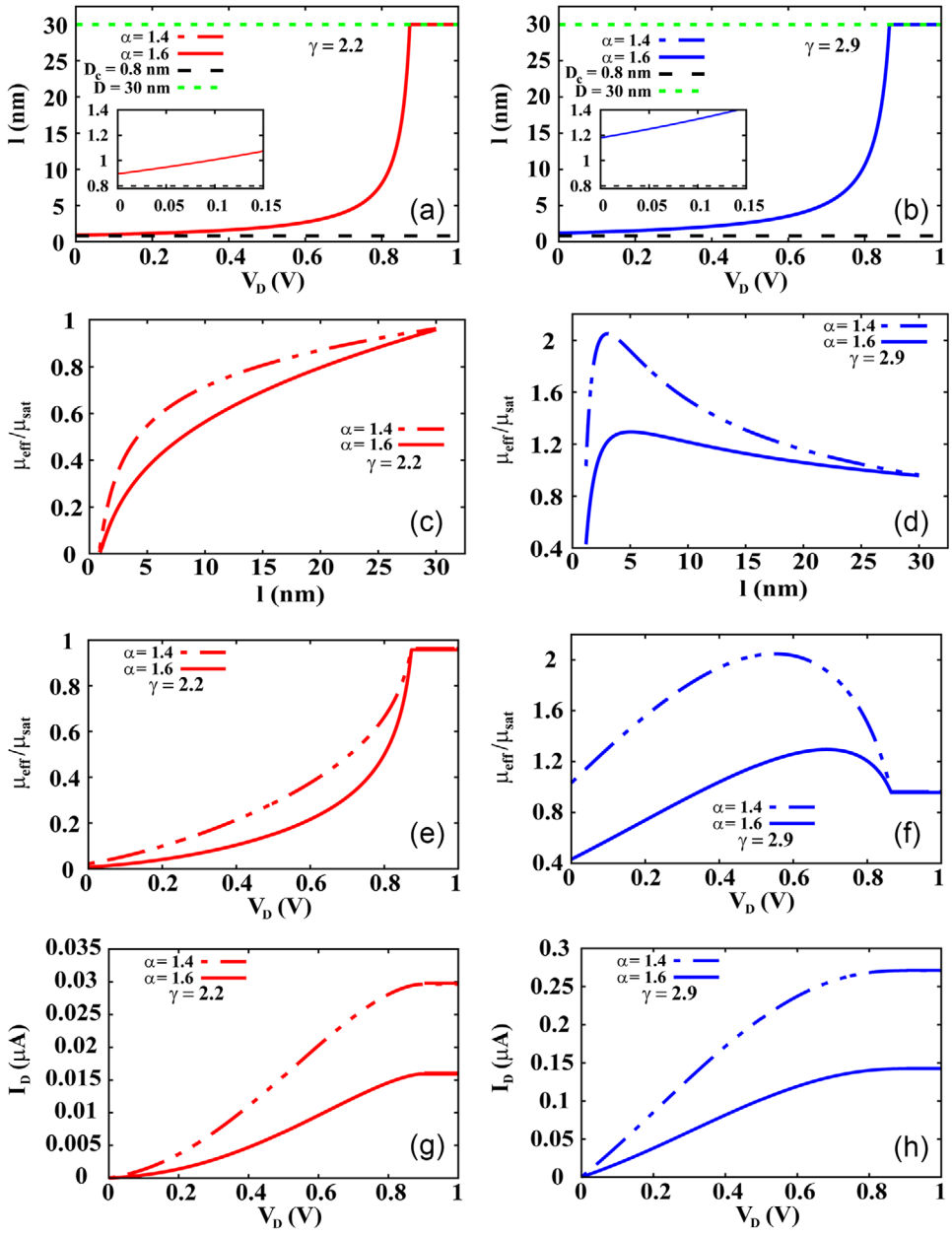

Figure 2. Electrolyte-gated transistor behaviors for 2D percolation transport (2D PT - dashed lines) and 3D percolation transport (3D PT - solid lines). a,b) Variation of the accumulation layer thickness $l = l_x$ as a function of V_D. Effective mobility normalized to the saturation one (μ_{eff}/μ_{sat}) as a function of c,d) l and e,f) V_D. h) Output curve (I_D–V_D). The transistors parameters used for this simulations are: $\alpha = 1.4$ for 2D PT and $\alpha = 1.6$ for 3D PT, $D = 30$ nm, $D_c = 0.8$ nm, $W = 1.0$ mm, $L = 30$ μm, $\kappa = 4.0$, $T = 300$ K, $V_G = 1.0$ V, $V_T = 0.1$ V and $\mu_{sat} = 1.23 \times 10^{-2}$cm^2 V^{-1} s^{-1}.

The **saturation regime** occurs when $V_D \geq V_{sat}$. Under this regime the drain current is

$$I_{D,sat} = I_D(V'', V_{sat}) + \frac{\mu_{sat} C_i W}{L}\left(\frac{D - D_c}{D}\right)^{\alpha}\frac{V_{tr}^2}{2} \quad (9)$$

where $I_D(V'', V_{sat})$ is the current given by Equation (6) with $V_D = V_{sat}$.

3. Results

Through the proposed model, we effortlessly analyzed some phenomena not easily obtained experimentally. **Figure 2** summarizes the first results, where the parameters are assumed to have values close to a typical EGOFETs.[12–14] It was compared the transistor behavior under 2D percolation transport (PT) regime (dashed lines) and 3D one (solid lines). The 2D PT can occur when the electronic coupling between states belonging to the same layer is higher compared to the coupling between states belonging

to adjacent layers of the semiconductor film. In this situation, the in-plane percolation paths are formed with higher probability. The charge carriers tend then to flow along the same plane of the semiconductor film. For the 3D PT, however, the in-plane and inter-plane percolation paths can occur with the same probability since the electronic coupling between states of the same layer is comparable to the coupling between states of adjacent layers. Here, the main parameter to make a distinction between an OFET and an EGOFET is the capacitance per unit area (C_i). The chosen value used was $C_i = 1.0\,\mu\text{F cm}^{-2}$, since values around 1.0 to 10 μF cm^{-2} are typically measured for EGOFETs.

First, the graphs from the left column side in Figure 2 will be discussed, considering $\gamma = 2.2$ represented by red curves. Figure 2a shows the accumulation thickness versus the applied drain voltage ($l \times V_D$). The green dashed curve indicates a semiconductor film thickness D and the black dashed one shows the critical percolation thickness D_c. At zero volts is the grounded source electrode ($V(x = 0) = 0$ V) and at $V(x = L)$=V_D= 1 V is the drain electrode position. The result shows that l is non-constant along the channel length and does not extend along all the semiconductor thickness until ≈ 0.85 V, under the simulated parameters. Close to the source electrode, the accumulation layer has just a few nanometers (see inset) and it reaches the thickness D close to the drain. If the same simulation is repeated just changing the C_i value to one similar to that observed in OFETs (≈ nF cm^{-2}), $l = D$ thickness for all the channel length (see Supporting Information). It proves that the analysis of the accumulation layer thickness is quite relevant for electrolyte-gated transistors due to its high C_i.

The graphs (c) and (e) in Figure 2 present the normalized ratio of $\mu_{\text{eff}}/\mu_{\text{sat}}$ as a function of l and V_D, respectively. The effective mobility (μ_{eff}) shows a non-constant range profile for all the curves, since it depends on the accumulation layer thickness l. The mobility approaches to μ_{sat} after reaching the condition $l = D$. The range where μ_{eff} profile increases is attributed to the percolation regime where mobility increases with the rise of percolation paths.[8] When μ_{eff} reaches its saturation, it means that the accumulation layer is a constant ($l = D$) and the traps do not present more dependence on the transport. Most of the region where the μ_{eff} is non-constant, it is equivalent to the linear field effect mobility (μ_{lin}).

The output curves in Figure 2g have two interesting results to be highlighted: i), influence of percolation transport and ii) nonlinear behavior of the output curve for lower V_D range. Considering (i), the influence of percolation transport: when the α parameter is varied, it is observed that the highest current intensity occurs for lower α, which means it is observed a higher current for 2D PT. It occurs since the 2D PT has lower degrees of freedom than the 3D PT regime. The transport in 3D can occurs along the plane film and also inter-plane, increasing the path length taken by the charge carriers along the channel. Indeed a considerably fraction of this length can be along the y-direction. Since the effective mobility derives from the effective charge's displacement along the x-direction, the output current has a lower intensity in the 3D PT regime (despite the higher degree of conducting possibilities). The same explanation also justifies the difference among the intensities of the effective mobility in the graphs (c) and (e) in Figure 2. Considering (ii), even though the present theoretical development was based on ohmic contacts,[8] a non-linear behavior was observed in the output curve for lower V_D range. This profile is frequently attributed to non-ohmic contacts.[15,16] In the present model, such behavior appears for the range of $\alpha \geq \gamma - 1$ which means that the percolation transport prevails over the trap-limited transport to determine the effective mobility. Since close to the source the accumulation thickness (l) is quite thin (Figure 2a), the probability that the charge carrier will reach a percolation pathway is lower in this region. Consequently, the film resistivity tends to be higher in the vicinity of the source which behaves like a contact resistance. Looking back to Figure 2e, for the equivalent V_D range analysis the μ_{eff} is quite low, which also reduces the output current intensity. Therefore, the output curve parabolic profile can be attributed to the injection limited current due to the very thin accumulation thickness close to the source along with a relevant amount of traps right after the injection interface. Such physical explanation to the non-ohmic output curve behavior at low V_D from a theoretical point of view is a novelty.

The right column graphs in Figure 2 depict an analogous simulation to the left one, but now for $\gamma = 2.9$, represented by blue curves. This higher γ's value simulate a higher amount of traps into the semiconductor in comparison to the previous analysis. The accumulation thickness as a function of V_D in the Figure 2b does not depict relevant changes in comparison to Figure 2a. In the Figure 2d,f, the effective mobility normalized to the μ_{sat} reaches values higher than one. It means that the linear field effect mobility (μ_{lin}) is higher than the saturation one (μ_{sat}). Figure 2d,f can be analyzed in the view of three regimes: i) Percolation regime, where the mobility increases due to the rise of percolation paths; ii) Bulk transport, where the mobility intensity decreases with the effective thickness rising along many monolayers,[8] resulting in a lower net electric field intensity leading to a lower average charge carriers velocity; iii) Still bulk transport, but now with a constant μ_{eff} that occurs when $l = D$ along with the fact that there is no longer any influence of the traps. Figure 2h shows the typical behavior of an output curve with a linear regime followed by saturation.

Interestingly, the current intensity depends on the kind of percolation transport: 2D or 3D, modeled when α parameter is changed. **Figure 3**a,b shows the output and transfer curves, respectively, for different α's but keeping all other parameters constant. In the output curve, the typical linear and saturation regimes are observed and the current intensity decreases for increasing α values. The dash double-dot lines depict output curves under 2D PT range and the solid-lines for 3D one. In the transfer curve (Figure 3b), relevant profiles changes are observed. While for $\alpha = 1$ the current is still modulating when $V_G = 1$ V, providing us the information that a higher V_G will still increase the on-off ratio, for example, for $\alpha = 1.6$ the maximum modulation was already reached for $V_G = 1$ V with a lower current intensity.

As showed before, as higher is the voltage V_D, thicker will be the accumulation layer thickness (see graphs from Figure 2a,b). It means that a transition among growing values of α can occurs under a V_D sweep, whose transient depends on the morphology of the film, not being possible to have a universal model for predicting this transition. The graph from Figure 3c depicts such situation where: $\alpha = 1.3$ from $V_D = 0.0$ V up to 0.2 V and, $\alpha = 1.6$ from $V_D = 0.8$ V up to 1.0 V. We supposed to have an α transient from 1.3 to 1.6 with step of 0.025 for every 0.05 V in V_D, for the drain voltage range of 0.2 up to 0.8 V. In this way, we manually

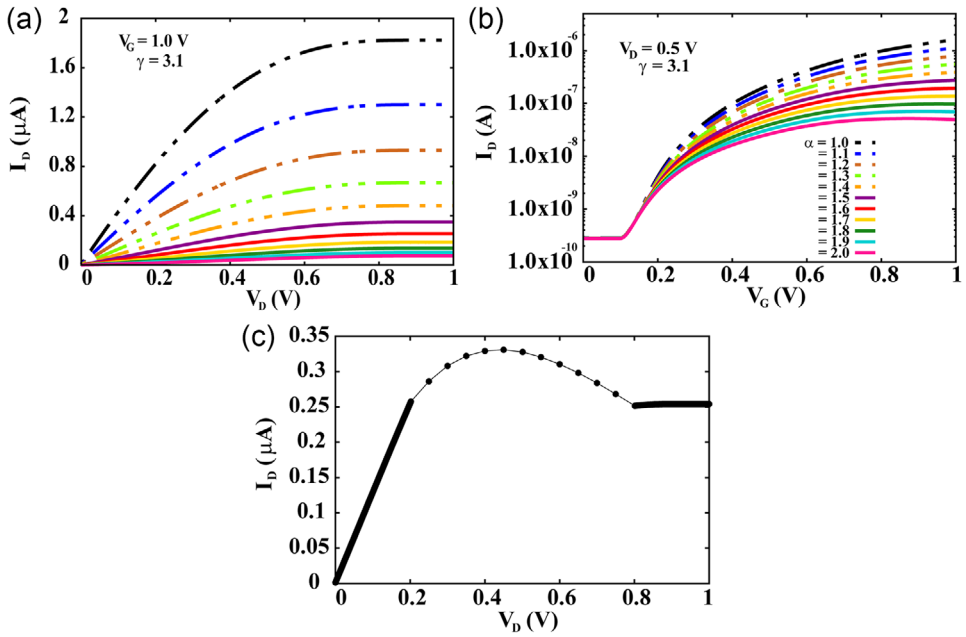

Figure 3. a) Output and b) transfer curves for a percolation transport in 2D (dashed lines) and a percolation transport in 3D (solid lines), where $\gamma = 3.1$. The current intensity for α values equivalent to 2D transport is higher than for 3D case. c) Hypothetical transition from $\alpha = 1.3$ to $\alpha = 1.6$, where α has a step of 0.025 every 0.05 V in V_D. Here $\gamma = 3.1$, $V_D = 1.0$ V and $V_T = 0.1$ V.

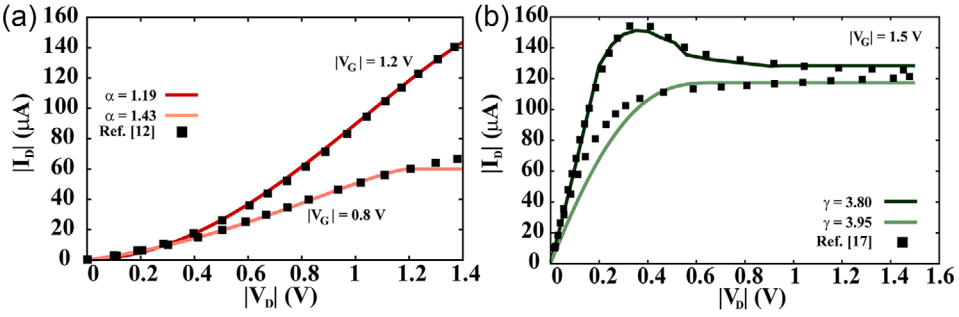

Figure 4. a) Experimental data (solid square dots) and theoretical fitting (solid lines) from an EGOFET output curves using the experimental parameters[12]: $|V_G| = 1.2$ V and $|V_G| = 0.8$ V. The theoretical variable parameter: $\alpha = 1.19$ for dark red and $\alpha = 1.43$ for light red. b) Theoretical fit on experimental data from an OECT output curve,[17] considering a transient from $\alpha = 1.375$ to $\alpha = 1.600$, for $|V_G| = 1.5$ V, $|V_T| = 0.5$ V and $\gamma = 3.8$ (dark green) to forward part of the cyclic measurement. For the backward cycle (light green), it was used $\alpha = 1.6$, $|V_T| = 0.8$ V, $\gamma = 3.95$.

extract each point that compose this region of the curve to illustrate such a situation. Due to the chosen α values, it represents a transition from 2D to 3D PT where a protuberance/lump is observed between the linear to the saturation typical regimes. Such profile has already been reported in experimental works but it has not yet been described using a 2D to 3D PT transition model. Such lump profile can also appear for α variation among just 2D PT range ($\alpha = 1$ to 1.4) or just 3D one ($\alpha = 1.5$ to 2).It is important to note that, from the set of parameters provided by the fit based on the present model, even a microscopic analysis is made to understand some typically observed experimental behaviors.

4. Experimental Fit

In the literature it is possible to find some papers reporting non-ohmic shaped output curves despite ohmic contacts. **Figure 4**a shows our model theoretical simulation fit (solid line) performed on the output curves from the experimental data of ref. [12] (solid square dots). The device is a poly-electrolyte-gated OFET depicting a non-linear behavior for low V_D range, whose structure is: Ti-Au/P3HT/P(VPA-AA)/Au and the used parameters on the modeling were extracted from the experimental measurements[12]: $V_T = 0.4$ V and $C_i = 1.0\ \mu$F cm^{-2}, while the channel dimensions are $W = 15$ mm, $L = 2\ \mu$m, and $D = 30$ nm. The theoretical parameters are: $\alpha = 1.19$ (for $|V_G| = 1.2$ V, dark red line) and $\alpha = 1.43$ (for $|V_G| = 0.8$ V, light red line), $\kappa = 4.0$, $T = 300$ K, $D_c = 0.4$ nm, $\mu_{sat} = 0.2$ cm^2 V^{-1} s^{-1} and $\gamma = 1.8$. Since α is related to a depth of percolation path, it seems coherent that this parameter changes depending on V_G, once a higher gate voltage produces a higher electric field intensity and a thinner accumulation layer thickness at the interface. Therefore, we assume a lower α for higher V_G (and vice-versa) that results in a good fitting for both curves. For the light red line fit, there is no agreement between experimental and theoretical data for $V_D > |1.2|$ V. From our

simulation, this curve must saturate after ≈ 1.2 V, since it was used the extracted experimental $V_T = +0.4$ V and therefore we do not interpret it as an inappropriate adjustment. From this fit, microscopic parameters were obtained: γ which indicates a narrower Gaussian distribution of states and α which is attributed to 2D percolation transport profile.

The experimental data in Figure 4b is from a polyelectrolyte-gated organic thin-film transistors with structure: Au/P3CPT/P(VPA-AA)/Ti[17] with a clockwise cyclic curve. The theoretical fit was separately simulated for the forward measure (dark green solid line) and backward one (light green solid line). The authors of the experimental work analyzed the transistor mode of operation considering ions diffusion into the channel, that is, it operates as an organic electrochemical transistor (OECT). The experimental data[17] and theoretical parameters used were: $W = 1$ mm, $L = 3\,\mu$m, and $D = 30$ nm, $C_i = 4\,\mu$F cm^{-}2, $|V_G| = 1.5$ V and $|V_T| = 0.5$ V, $\kappa = 4.5$, $T = 300$ K, $D_c = 0.3$ nm, $\mu_{sat} = 6.5 \times 10^{-3}$cm^2 V^{-1} s^{-1} and $\gamma = 3.8$. To fit the protuberance profile between the linear and saturation regimes in the forward measure, it was considered a transient from $\alpha = 1.375$ up to $\alpha = 1.600$ in the region where the lump profile appears, resulting in a very good fit.

Despite the present model is fully based on the description of transistors based on field effect modulation like FETs, OFETs, or EGOFETs, we successfully fitted an OECT describing a non-ideal behavior where a lump appears between the linear and saturation regimes. The interpretation given to this fit is that when ions diffuse into the channel resulting in ionic doping, they generate a new electrical rearrangement which can be represented by an equivalent local field effect. This distribution of charges and ions is found along the accumulation layer that can extend close to the surface of the semiconductor or along its entire volume. Similar situation, of non-constant hole and cation concentrations along the channel, has already been described in the literature where the cation concentration increases exponentially toward the drain electrode.[10] However, our model quantifies this field effect generated by both charge carriers and ions, without making a distinction between each one and providing a net result of their contributions. Therefore, while some OECTs models propose to quantify a volumetric capacitance generated by the diffusion of ions inside the channel, the present model shows that a simplified analysis is enough to quantify the field effect generated by both charges and ions along the accumulation layer.

It is important to note that after obtaining the simulation parameters from the output curve fitting, it is possible to infer information not provided by the experimental characterization by plotting the graphs: $l \times V_D$; $\mu_{eff}/\mu_{sat} \times V_D$; and electric field intensity as a function of V_D or y, where y represents the channel thickness direction. The mentioned graphs analysis are depicted in Supporting Information using the parameters from the OECT fit simulation, Figure 4b. It shows that the accumulation layer reaches the semiconductor thickness at $V_D \approx$ 1 V. The μ_{eff} as a function of V_D has three regimes: increasing, decreasing and saturation, whose description of the physical phenomena are the same as those attributed to the Figure 2f. According to our model, in the range of the linear regime μ_{lin} it has a maximum value at $V_D \approx$ 0.4 V and $\alpha = 1.375$, almost 100 times higher than μ_{sat}, and at $V_D \approx$ 0.8 V with $\alpha = 1.600$ it is almost 20 times higher than μ_{sat}. In a parallel analysis of the mobility intensity on the graph of the electric field intensity along the accumulation layer, it is possible to perceive a region with an electric field a 100 times higher in a region that goes from the source to part of the channel length, reducing closer to the drain. This region with such higher electric field intensity is attributed to the region with the highest concentration of ions diffused into the channel. In summary, this high concentration of charges and ions when there is a very thin accumulation layer results in such a very high field effect mobility. The in-homogeneity of ions distribution along the channel has already been shown through a non-quantitative measurement named as simple $I \times V$ curve in the literature,[14] where the curve profile is asymmetric showing that ions are not equally distributed within the channel under certain conditions. For instance, such analysis indicates the region at the semiconductor/dielectric interface where the diffusion of ions to the channel is more favorable. It is situated in the vicinity of the grounded electrode due to the higher intensity of the electric field in this part of the channel. The interpretation of the non-homogeneity described here is dependent only on the applied voltage and transistor's geometry, assuming that the equilibrium due to the transient time from ions movement has already been reached.

For the backward cyclic measure direction (from Figure 4b), it was necessary to increase the values of two parameter: $\gamma = 3.95$ and $V_T = 0.8$ V. Since ions have been diffused during the measurement performance it is expected that the properties of the semiconductor/electrolyte interface are changed. In this case, the new parameters provide the information that there are more traps close do the interface and a broader Gaussian distribution that is coherent with the presence of ions into the channel.

The **Figure 5** and following sentences correlate some of the parameters used in the model's simulation with a practical vision in the development of transistors. Figure 5a,b, illustrates the top view of the source/channel/drain structure where the colored parts along the channel represent the semiconductor film that has low electrical resistance and blank parts depicting islands of high resistance. The limit of each illustration is a comparison of the D_c with l. D_c is the parameter that describes the minimum thickness of the semiconductor that promotes at least one percolation path along the source and drain electrodes, as depicted in the Figure 5a with a green arrow. Figure 5c,d shows a side view of the transistor's structure with a grained profile semiconductor. The solid black line represents the accumulation layer that has a very thin thickness close to the source and it reaches the full thickness of the semiconductor (D) close to the drain. When $l < D_c$ (Figure 5b,d), there is no conduction along the channel. For $l > D_c$ (Figure 5a,b), there is conduction along the channel and the current intensity has dependence with l thickness.

The D_c parameter is directly related to the morphology of the semiconductor's surface. In a macroscopic view, D_c can be described as the roughness at the contact interface between the gate dielectric and the semiconductor. For a very thin organic semiconductor's film, this roughness can produce regions where the semiconductor coverage forms low resistance islands isolated by highly resistive domains formed by dielectric material (see Figure 5).

The α parameter describes the percolation transport regime. This parameter is essentially related to the topology of the network (produced by percolation pathways) that link low resistance

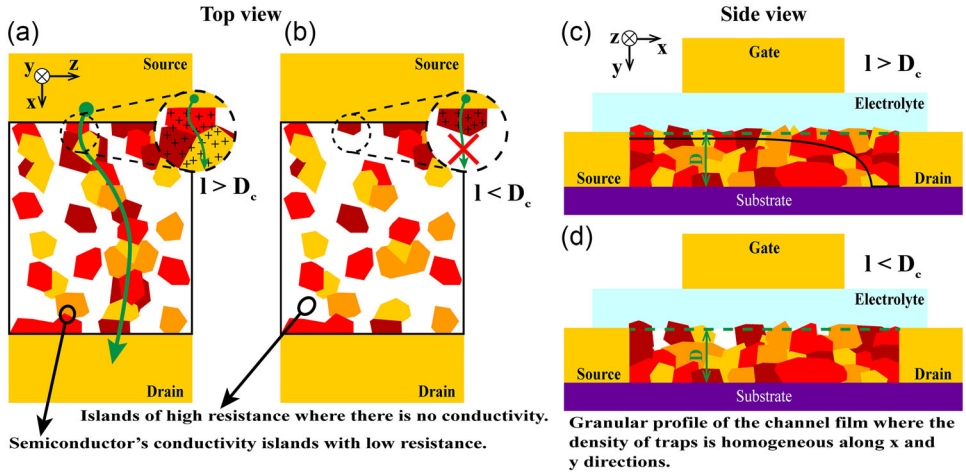

Figure 5. a,b) Top view of the source/channel/drain structure where the colored parts along the channel represent the semiconductor film with low resistance and blank parts depict islands of high resistance. The green arrow represents one percolation path between source and drain. c,d) Side view of the transistor's structure with a grained profile semiconductor. The solid black line represents the accumulation layer thickness (l), close to the semiconductor/dielectric interface. Green dotted line represents the semiconductor thickness (D).

regions/islands distributed along the source and drain electrodes (see Figure 5a,b).

The γ parameter describes the energetic trap depth and it depends on the morphology of the semiconductor's film. It also depends on intrinsic details of the electronic couple between molecules. Many factors can influence the morphology like: the roughness from the previous layer deposition, the solvent when film is prepared from solution, temperature deposition and/or annealing process, etc. It means that the same polymer film deposited in different laboratories, solution processes, deposition methods and/or ambient conditions can result in different values of γ parameter. In addition, γ parameter can be associated to the degree of off-diagonal disorder in the organic semiconductor's film. The analysis derived from the experimental fit (see Figure 4b), suggests that this parameter can also be associated to the presence of an hysteresis in output current curves. That is, when ions diffuse into the semiconductor, it can promote an increase in morphological disorder due to the electrostatic forces. Then, new trap states energy shifts can lead to higher values of γ.

Still from experimental fit analysis (Figure 4b), the increasing change in α value is able to fit the lump on the output curve, it means that the kind of percolation path changes with the voltage variation. But it is important to emphasize that making an ascending (or descending) sweep in the α value will not always generate non-ideal profiles in the output curve. Nonetheless, α value variations always interfere in the intensity of the output current. Therefore, this parameter can also be responsible for the formation of hysteresis in the output current.

Some literature attributes the hysteresis in the output current (transfer and characteristic curves) to the slow drift time of the ions, which in fact can occur. Consequently, researchers measuring those curves must always be aware that the device's response might depend on kinetic effects related to charges and ions. Hence appropriate scan rate measurements are fundamental to discard such effects in the transfer and output curves. Make the sweep rate of electrical measurements explicit in EGOFETs and, mainly in OECTs, should be mandatory in experimental works for understanding hysteresis and other phenomena observed in the typical electrical characterization of EGTs. From the present model, the hysteresis can be attributed to changes in the type of percolation transport (α) and/or with the energetic depth of the exponential distribution of the shallow traps (γ).

Finally, This model proved capable of bringing physical interpretations of the operating modes of EGOFETs and OECTs. In addition to extracting typical transistor parameters, microscopic information is provided from the theoretical adjustment, inferring information not obtained only through electrical measurements.

5. Conclusion

A theoretical model was proposed for the charge carriers transport in EGTs considering the influence of a shallow exponential traps distribution in the semiconductor and 2D or 3D PT. An important inference of the model is that the influence of the high capacitance per unit area formed at the interface semiconductor/electrolyte dielectric gate promotes changes on the thickness of the accumulation layer. The accumulation thickness does not necessarily extend along the entire semiconductor thickness. This influence was inserted into the model in the effective mobility parameter ($\mu_{\text{eff}}(l)$). It is possible to analyze both EGOFETs and OECTs modes of operation in steady-state and extract parameters as: field effect mobility; γ that correlates to the exponential energetic depth of traps; and α that provides if 2D or 3D PT occurs. These parameters were used to simulate: i) accumulation layer thickness profile and ii) effective mobility, both as function of V_D. The last provides an interpretation if the linear field effect mobility μ_{lin} has a non-constant behavior and if it is lower or higher than μ_{sat}. For an EGOFET, the accumulation layer thickness describes the charge carriers distribution along the channel length, while for OECTs it represents the distribution of both charge

carriers and diffused ions. The present model considers just the net electric field formed by the distribution of both charges carriers and ions, without distinguishing their contributions.

Two theoretical/experimental fits were demonstrated: i) the non-linear behavior for low V_D in an EGOFET output curve considering an ohmic contact. Such profile is attributed to the very thin effective thickness (l) close to the source together with the influence of the exponential traps presence and this interpretation extracted from a model simulation is a novelty; ii) the adjustment of the lump behavior between the linear and saturation regimes observed on some EGTs output curves. The lump profile was attributed to a transient from 2D to 3D PT under the analyzed parameters that were reasonable estimates. Based on these two successful adjustments, the proposed model can be considered general to be applied in EGTs operating as EGOFET or OECT.

Supporting Information

Supporting Information is available from the Wiley Online Library or from the author.

Acknowledgements

The authors thank to the Coordenação de Aperfeiçoamento de Pessoal de Nível Superior – Brasil (CAPES) – Finance Code 001 and M.K. thanks to CNPq (grant 310251/2021-4).

Conflict of Interest

The authors declare no conflict of interest.

Data Availability Statement

The data that support the findings of this study are available from the corresponding author upon reasonable request.

Keywords

charge carriers transport modeling, electrolyte-gated transistor model, electrolyte-gated organic field effect transistors, general electrolyte-gated transistors model, organic electrochemical transistors

Received: November 18, 2022
Revised: February 10, 2023
Published online: March 12, 2023

[1] G. Hadziioannou, P. van Hutten, *Semiconducting Polymers: Chemistry, Physics and Engineering*, Wiley, Weinheim **2000**.
[2] G. Horowitz, in *Organic Electronics* (Eds: T. Grasser, G. Meller, L. Li), Springer Berlin Heidelberg, Berlin, Heidelberg **2010**, pp. 113–153.
[3] N. Delavari, K. Tybrandt, M. Berggren, B. Piro, V. Noël, G. Mattana, I. Zozoulenko, *J. Phys. D: Appl. Phys.* **2021**, *54*, 415101.
[4] D. A. Bernards, G. G. Malliaras, *Adv. Funct. Mater.* **2007**, *17*, 3538.
[5] Z. Bao, J. Locklin, *Organic Field-Effect Transistors*, 1st ed., Optical Science and Engineering, CRC Press, Boca Raton, FL **2007**.
[6] P. R. Paudel, M. Skowrons, D. Dahal, R. K. R. Krishnan, B. Lüssem, *Adv. Theory Simul.* **2022**, *5*, 2100563.
[7] G. C. Faria, D. T. Duong, A. Salleo, *Org. Electron.* **2017**, *45*, 215.
[8] M. Koehler, K. F. Seidel, *Phys. Rev. B* **2010**, *81*, 085305.
[9] F. Dinelli, M. Murgia, P. Levy, M. Cavallini, F. Biscarini, D. M. d. Leeuw, *Phys. Rev. Lett.* **2004**, *92*, 116802.
[10] V. Kaphle, P. R. Paudel, D. Dahal, R. K. Radha Krishnan, B. Lüssem, *Nat. Commun.* **2020**, *11*, 2515.
[11] M. Weis, *J. Appl. Phys.* **2012**, *111*, 054506.
[12] L. Kergoat, L. Herlogsson, B. Piro, M. C. Pham, G. Horowitz, X. Crispin, M. Berggren, *Proc. Natl. Acad. Sci. USA* **2012**, *109*, 8394.
[13] L. Kergoat, L. Herlogsson, D. Braga, B. Piro, M.-C. Pham, X. Crispin, M. Berggren, G. Horowitz, *Adv. Mater.* **2010**, *22*, 2565.
[14] E. A. de Moura, M. Luginieski, J. P. M. Serbena, K. F. Seidel, *J. Appl. Phys.* **2021**, *129*, 154502.
[15] M. Waldrip, O. D. Jurchescu, D. J. Gundlach, E. G. Bittle, *Adv. Funct. Mater.* **2020**, *30*, 1904576.
[16] C. Liu, T. Minari, Y. Xu, B. ru Yang, H.-X. Chen, Q. Ke, X. Liu, H. C. Hsiao, C. Y. Lee, Y.-Y. Noh, *Org. Electron.* **2015**, *27*, 253.
[17] A. Laiho, L. Herlogsson, R. Forchheimer, X. Crispin, M. Berggren, *Proc. Natl. Acad. Sci. USA* **2011**, *108*, 15069.